ELSEVIER

Contents lists available at ScienceDirect

Chemosphere

journal homepage: www.elsevier.com/locate/chemosphere





Algal ciguatoxin identified as source of ciguatera poisoning in the Caribbean

Elizabeth M. Mudge ^{a,*}, Christopher O. Miles ^a, Lada Ivanova ^b, Silvio Uhlig ^b, Keiana S. James ^{c,d}, Deana L. Erdner ^e, Christiane K. Fæste ^b, Pearse McCarron ^a, Alison Robertson ^{c,d,**}

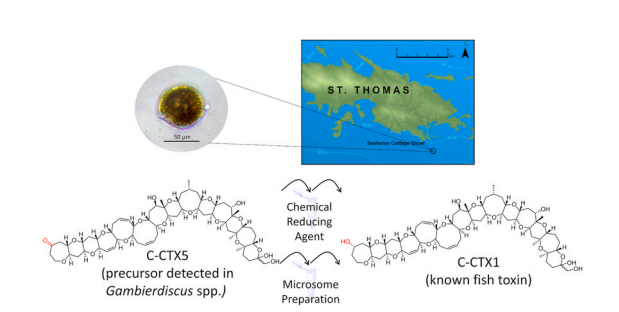
- ^a Biotoxin Metrology, National Research Council, 1411 Oxford Street, Halifax, NS, B3H 3Z1, Canada
- ^b Chemistry and Toxinology Research Group, Norwegian Veterinary Institute, P.O. Box 64, 1431 Ås, Norway
- ^c School of Marine & Environmental Sciences, University of South Alabama, 600 Clinic Drive, AL, 36688, USA
- ^d Marine Ecotoxicology Group, Dauphin Island Sea Lab, 101 Bienville Blvd, Dauphin Island, Dauphin Island, AL, 36528, USA
- ^e Marine Science Institute, University of Texas at Austin, 750 Channel View Dr, Port Aransas, TX, 78373, USA

HIGHLIGHTS

Gambierdiscus silvae and G. caribeaus isolated in Caribbean with CTX-like activity.

- Putative C-CTX detected about 20 × higher abundance to C-CTX1/2 in G silvage
- C-CTX5 structure confirmed with chemical and enzymatic conversions to known C-CTXs.
- Confirmed Caribbean CTX (C-CTX5) as precursor in microalgal source.

GRAPHICAL ABSTRACT



ARTICLE INFO

Handling editor: J. de Boer

Keywords:
LC-HRMS
Gambierdiscus silvae
Gambierdiscus caribaeus
Caribbean ciguatoxin
Ciguatera poisoning
Voltage-gated sodium channel
In vitro hepatic biotransformation

$A\ B\ S\ T\ R\ A\ C\ T$

Ciguatera poisoning (CP) is a severe seafood-borne disease, caused by the consumption of reef fish contaminated with Caribbean ciguatoxins (C-CTXs) in the Caribbean and tropical Atlantic. However, C-CTXs have not been identified from their presumed algal source, so the relationship to the CTXs in fish causing illness remains unknown. This has hindered the development of detection methods, diagnostics, monitoring programs, and limited fundamental knowledge on the environmental factors that regulate C-CTX production. In this study, *in vitro* and chemical techniques were applied to unambiguously identify a novel C-CTX analogue, C-CTX5, from *Gambier-discus silvae* and *Gambierdiscus caribaeus* strains from the Caribbean. Metabolism *in vitro* by fish liver microsomes converted algal C-CTX5 into C-CTX1/2, the dominant CTX in ciguatoxic fish from the Caribbean. Furthermore, C-CTX5 from *G. silvae* was confirmed to have voltage-gated sodium-channel-specific activity. This finding is crucial for risk assessment, understanding the fate of C-CTXs in food webs, and is a prerequisite for development of effective analytical methods and monitoring programs. The identification of an algal precursor produced by two *Gambierdiscus* species is a major breakthrough for ciguatera research that will foster major advances in this important seafood safety issue.

https://doi.org/10.1016/j.chemosphere.2023.138659

Received 8 February 2023; Received in revised form 6 April 2023; Accepted 8 April 2023 Available online 10 April 2023

^{*} Corresponding author.

^{**} Corresponding author. School of Marine and Environmental Sciences, University of South Alabama, 600 Clinic Drive, STE 300, Mobile, Alabama, 36688, USA. *E-mail addresses*: Elizabeth.mudge@nrc-cnrc.gc.ca (E.M. Mudge), arobertson@disl.org (A. Robertson).

1. Introduction

Ciguatera poisoning (CP) is a global disease that disproportionately affects coastal communities subsisting on local seafood resources in tropical and subtropical regions such as the Pacific Ocean, Indian Ocean and Caribbean Sea, with several emerging regions including Macaronesia, the Eastern Mediterranean and the Gulf of Mexico (Chinain et al., 2021). Historical data and global occurrences of ciguatoxins have been reviewed in Chinain et al. (2021) and the FAO and WHO (2020) expert report on CP. In the Caribbean, up to 5% of island populations have been estimated to be affected, causing significant socioeconomic and health impacts (Morris et al., 1982; Pottier et al., 2001; Azziz--Baumgartner et al., 2012; Radke et al., 2013). While these communities bear the direct impacts of CP on seafood safety and human health, highly productive tropical waters also provide rich commercial fisheries, and fish products that are exported internationally have resulted in CP outbreaks in more temperate regions where CP is not endemic (Villareal et al., 2006; Graber et al., 2013; Epelboin et al., 2014; Muecke et al., 2015; Friedemann, 2016; Loeffler et al., 2022). CP is caused by the consumption of seafood contaminated with ciguatoxins (CTXs), a group of toxic polyethers that bind to voltage-gated sodium channels leading to depolarization of cells (Dechraoui et al., 1999). Several CTXs have been characterized from the Caribbean in fish (Lewis et al., 1998; Kryuchkov et al., 2020) and in microalgae, invertebrates and fish from the Pacific (Murata et al., 1990; Lewis et al., 1993; Satake et al., 1993, 1996, 1998), with variations in structure and toxicity. Significant advances in understanding the accumulation and biotransformation of CTXs in fish in the Pacific region (Ikehara et al., 2017; FAO and WHO, 2020) have been made since the identification of the benthic dinoflagellate Gambierdiscus polynesiensis that produce Pacific CTXs (Satake et al., 1993, 1996; Chinain et al., 2010; Rhodes et al., 2014; Longo et al., 2019; Darius et al., 2022). While many other species of Gambierdiscus are found in the marine reef ecosystems (Litaker et al., 2010; Tester et al., 2020), G. polynesiensis this is the only species of Gambierdiscus confirmed to produce Pacific CTXs. G. polynesiensis meets the criteria proposed by Holmes et al. (1994) to be considered a 'CTX-producing super-strain', where it was hypothesized that only some Gambierdiscus are genetically capable of producing CTXs and therefore, highly toxic Gambierdiscus strains must be present but may not dominate the microalgal

assemblages in the reef ecosystems in order for CTXs to accumulate in the marine food web (McMillan et al., 1986; Holmes et al., 1991, 1994; Caillaud et al., 2010; Liefer et al., 2021). The toxicity of G. polynesiensis has been reported to range from 0.7 to 20.9 pg CTX3C equivalents (eq.) cell⁻¹ depending on the strain, origin, and detection method (Chinain et al., 2010; Pawlowiez et al., 2013; Rhodes et al., 2014; Darius et al., 2018, 2022). However, while many studies have reported in vitro toxicity associated with several Gambierdiscus species in the Caribbean (Lewis et al., 2016; Litaker et al., 2017; Liefer et al., 2021), an algal source of Caribbean CTXs (C-CTXs) has not yet been identified. Several Gambierdiscus spp. in the Caribbean, including G. caribaeus, G. carolinianus, G. belizeanus, and G. carpenteri, have been typically reported with low in vitro toxicities (e.g., G. caribaeus 0.6–1.3 fg CTX3C eq. $cell^{-1}$, G. carolinianus 0–1.0 fg CTX3C eq. $cell^{-1}$) (Litaker et al., 2017; Pisapia et al., 2017a; Díaz-Asencio et al., 2019). Some species like G. silvae and G. excentricus have been reported to have high in vitro toxicities based on functional assays (up to 4.8 pg C-CTX1 eq. cell⁻¹ for G. silvae (Robertson et al., 2018); and up to 1.4 pg CTX3C eq. cell⁻¹ for G. excentricus (Pisapia et al., 2017a)). Rossignoli et al. (2020) demonstrated that crude extracts of several cultures of *G. silvae* from the Canary Islands exhibited CTX-like activity in vitro and no non-specific cell death (cytotoxicity) was observed.

C-CTX1/2 (Fig. 1) is an equilibrating pair of large, heat-stable, ladder-shaped toxins composed of 14 polyether rings (Lewis et al., 1998) that rapidly interconvert through epimerization at a hemiketal at C-56 (Lewis et al., 1998; Kryuchkov et al., 2020). They are the dominant CTXs in fish from the Caribbean and Northeast Atlantic (Pottier et al., 2002a; Abraham et al., 2012; Estevez et al., 2020; Kryuchkov et al., 2020). Two presumed metabolites, C-CTX3 and C-CTX4 (Fig. 1), recently identified in kingfish (Scomberomorus cavalla) and great barracuda (Sphyraena barracuda), are analogues of C-CTX1/2 in which the hemiketal at C-56 has been reduced to a hydroxy group, converting them into a pair of non-equilibrating epimers that can be chromatographically separated (Kryuchkov et al., 2020). Isolation and characterization of CTXs from the Caribbean has been hampered by low yields of C-CTXs from fish tissue e.g., 51 kg of fish tissue was required to obtain \sim 150 µg of purified C-CTX1 for the original structure elucidation (Lewis et al., 1998). Other polyether compounds, including gambierones and maitotoxins, have been detected in Caribbean Gambierdiscus strains (Rodríguez et al.,

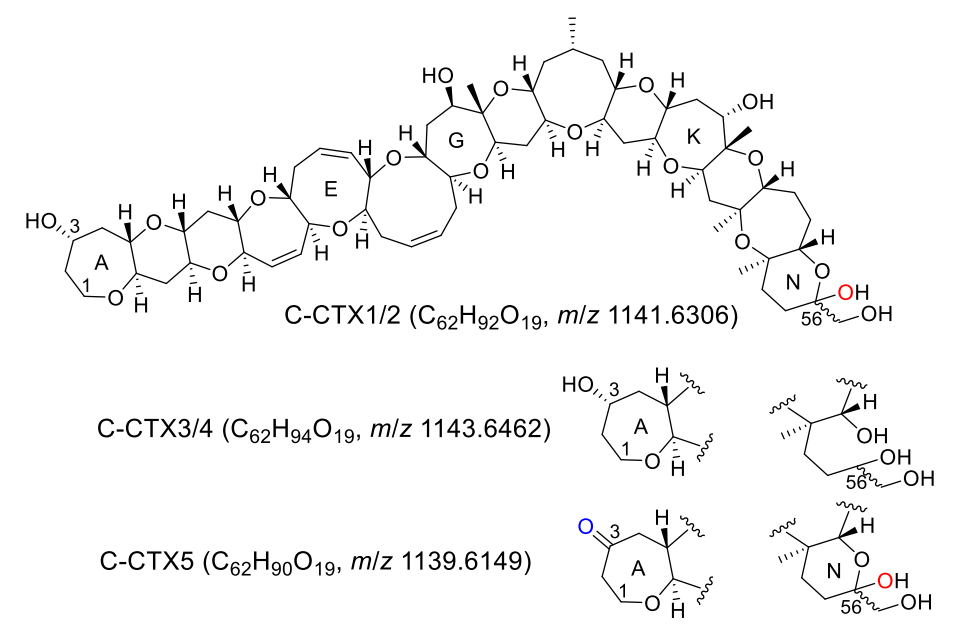


Fig. 1. Structures of the known Caribbean ciguatoxins C-CTX1 to C-CTX4 and the novel C-CTX5, along with their elemental formulae and the exact masses of their $[M+H]^+$ ions. Selected polyether rings A–N and carbons 1, 3, and 56 are marked, and the ketone and hemiketal oxygen atoms are coloured blue and red, respectively.

2015; Pisapia et al., 2017b; Boente-Juncal et al., 2019; Mazzola et al., 2019; Mudge et al., 2022b), but compounds with the C-CTX molecular backbone have not been reported. Despite significant risks to human health and the socioeconomic impacts of CP, as well as extensive field and analytical efforts on *Gambierdiscus* spp. over the 25 years since C-CTX1 was isolated, the algal source of C-CTXs remains unknown. This has severely hampered the development of methods for monitoring and toxin analysis, production of reference materials and, more broadly, improvement in CP management for seafood safety and community health.

The Island of St. Thomas in the U.S. Virgin Islands is a known hyperendemic region for ciguatera outbreaks (Morris et al., 1982; Tosteson, 1995; Radke et al., 2013). We hypothesized that *Gambierdiscus* spp. collected from this region that exhibited CTX-like *in vitro* might produce CTX precursors that could explain the origins of CP in the Caribbean. One *G. silvae* strain and two *G. caribaeus* strains that had been isolated from macroalgae collected from reefs surrounding St. Thomas, in the U. S. Virgin Islands had CTX-like Na_V activity *in vitro*, in the absence of non-specific activity. Based on these criteria, these *Gambierdiscus* strains were screened for known and unknown putative C-CTXs using liquid chromatography—high resolution mass spectrometry (LC—HRMS).

2. Material and methods

2.1. Reagents

Methanol (MeOH), acetone, n-hexane, acetonitrile (MeCN), chloroform, dimethyl sulfoxide (DMSO), and formic acid (~98%) were LC-MS grade from ThermoFisher Scientific (Ottawa, ON, Canada; Waltham, MA, USA). Dichloromethane was from Caledon Laboratories (Georgetown, ON, Canada). Reagent grade sodium metaperiodate (>99%), sodium borohydride (≥98%), sodium cyanoborohydride (95%), ouabain octahydrate, veratrine hydrochloride, reduced β -nicotinamide adenine dinucleotide 2'-phosphate tetrasodium salt hydrate (NADPH), β-nicotinamide adenine dinucleotide phosphate sodium salt hydrate (NADP⁺), HEPES sodium salt, p-glucose 6-phosphate sodium salt, p-glucose-6phosphate dehydrogenase from baker's yeast (Saccharomyces cerevisiae), MgSO₄, CaCl₂, hexadecyltrimethylammonium bromide (CTAB), and $0.22~\mu m$ PVDF spin filters were from Millipore-Sigma (Oakville, ON, Canada; St. Louis, MO). 3-(4,5-Dimethylthiazol-2-yl)-2,5-diphenyltetrazolium bromide (MTT) was from Alfa Aesar (Haverhill, MA, USA) and was prepared in sterile phosphate-buffered saline (PBS) from Millipore-Sigma (St. Louis, MO, USA). MgCl₂•6H₂O was from Honeywell Fluka (Bucharest, Romania). Adherent murine neuroblastoma cells (N2a; ATCC CCL-131) were from the American Tissue Culture Collection (ATCC; Manassas, VA, USA) and independent modified cell lines (i.e., desensitized to ouabain and veratrine (Loeffler et al., 2021)) were generated, authenticated and routinely tested for mycoplasma contamination as described in the Supplementary Information. $H_2^{18}O$ (97%) was from Cambridge Isotope Laboratories (Tewksbury, MA, USA). Distilled water was ultra-purified to 18.2 M Ω \times cm using Milli-Q (Millipore-Sigma) or Purelab Flex Veolia (Elga, Woodridge, IL, USA) water purification systems. CTX3C (100 ng) was from Wako Chemicals (Osaka, Japan) where two different lots were used (Wako-1, APK4222; Wako-2, TWJ6482) and prepared in MeOH (50 ng mL $^{-1}$). Gambierone (19.9 μ g mL⁻¹ in MeOH) was from CIFGA (Lugo, Spain), and 44-methylgambierone was from the Cawthron Institute (25 µg mL⁻¹ in MeOH; Nelson, New Zealand) and CIFGA (19.9 $\mu g \text{ mL}^{-1}$ in MeOH).

Methanolic extracts of fish collected from the Bastille Day Kingfish Tournament (St. Thomas, U.S. Virgin Islands, USA) on July 17, 2016, were used as reference materials due to their verified presence of C-CTX1/2 and C-CTX3/4, as described previously (Kryuchkov et al., 2020). Semi-purified C-CTX1/2 used to compare relative toxicity with C-CTX5 was prepared from *Sphyraena barracuda* and *Scomberomorus cavalla* collected from the U.S. Virgin Islands as previously reported (Mudge et al., 2022a). Sheepshead (*Archosargus probatocephalus*) were

collected from Mobile Bay, AL, USA and emerald parrotfish (*Nicholsina usta*) were from St. Andrews Bay, FL, USA. Collection permits, IACUC approvals, liver collection, and microsome preparation were as previously described (Gwinn et al., 2021).

2.2. Gambierdiscus spp. collection, isolation, culturing and identification

Dinoflagellate isolates were prepared from live samples collected in 2016, from *Dictyota* spp. in coastal waters south of St. Thomas, in the U. S. Virgin Islands, under approved scientific collection permits from the Virgin Islands Department of Fish and Wildlife (Lozano-Duque et al., 2018; Liefer et al., 2021). *Dictyota* spp. were collected by SCUBA divers (10–22 m depth) and placed into Ziplock bags with ambient seawater. The bags were vigorously shaken to dislodge the epiphytic cells, and the contents were sequentially filtered through 200 μ m and 20 μ m nylon sieves. Filtered (20 μ m, Nitex) site-specific seawater was added to the macroalgae and this process was repeated for a total of five cycles. The cells retained on the 20 μ m sieve were backflushed with 20 μ m filtered seawater and shipped overnight to the University of Texas Marine Science Institute UTMSI at Port Aransas, TX, USA. Cells were isolated, established as monocultures, and identified to species as previously described (Lozano-Duque et al., 2018).

Batch cultures of G. silvae (1602 SH-6) and G. caribaeus (BPAug08 and USVI-08) strains were grown in 1 L of natural seawater from the Gulf of Mexico that was adjusted to 36% salinity with ultrapure water, filtered through a 0.2 µm filter to remove particulates, and sterilized by autoclaving. It was enriched with Keller nutrients (Keller et al., 1987) with the following modifications (Kibler et al., 2012): no ammonium or Tris were added, and copper was omitted from the trace metal stock. Cultures were maintained at 25 °C under fluorescent light with an irradiance of ca. 100 μ mol photons m⁻² s⁻¹ (±10%) with a light:dark cycle of 12:12 h and harvested when they reached mid-to late-exponential phase. Immediately prior to sampling, the flasks were inverted several times and mixed on a vortex-mixer. For each culture flask, subsamples were removed and preserved with Lugol's iodine solution for determination of cell concentrations. Cell densities were determined using a 1-mL gridded Sedgewick-Rafter counting chamber under light microscopy. Replicate cell counts (n = 9 per strain) of cultures prior to harvest showed the mean and standard deviation for each as 1950 \pm 150 cells mL^{-1} for 1602 SH-6; 990 \pm 70 cells mL^{-1} for BPAug08, and $2080 \pm 90 \ cells \ mL^{-1}$ for USVI-08.

Species identification of the isolates was confirmed by DNA sequencing. Cells were collected onto a $5 \mu m$ pore size, 25 mm diameter nitex filter, and DNA was extracted using the CTAB method (Doyle and Doyle, 1987). Approximately 15 000 cells were collected for DNA extraction, and the concentration of the resulting DNA extract was adjusted to 5 ng μL^{-1} . The D1-D2 hypervariable region of the large subunit (LSU) rRNA was amplified using the primers D1R (5'-ACCCGCTGAATTTAAGCATA-3') and D2C (5'-CCTTGGTCC GTGTTTCAAGA-3') (Scholin et al., 1994). PCR amplification reactions (25 μL) contained ~5 ng template DNA, PCR buffer (500 mM KCl and 100 mM Tris HCl, pH 8.3), 0.25 mM of each dNTP, 0.5 μ M of D1R primer, $0.5~\mu\text{M}$ of D2C primer, and 0.625~units of Taq DNA Polymerase (Takara Taq Bio Inc, San Jose, CA, USA). PCR amplification was performed using an Eppendorf Mastercycler thermocycler (Enfield, CT, USA) as follows: 3 min denaturing at 95 °C (after 1–2 min at 94 °C, the cycle was paused to add the Taq), followed by 35 cycles of 30 s denaturing at 95 °C, 30 s annealing at 55 °C, 1 min elongation at 72 °C, and a final elongation for 10 min at 72 °C. Successful amplification was verified using 5 μL of each PCR reaction mixed with 2 μL of loading dye containing Midori Green Direct nucleic acid gel stain (Bulldog Bio, Portsmouth, NH, USA), checked by gel electrophoresis on 0.7% agarose (0.5 \times tris-borate-EDTA) and visualized under blue light (FastGene Imaging System, Bulldog Bio, Portsmouth, NH, USA).

PCR products were cloned using the TOPO TA system (Invitrogen Life Technologies, Carlsbad, CA, USA), according to manufacturer directions. Immediately after verification by electrophoresis, a 2 µL aliquot of the fresh PCR reaction was ligated into the linearized pCR4-TOPO vector as recommended, including salt. A 2 µL aliquot of the ligation reaction was used to transform TOP10 chemically competent cells, which were grown for 1 h without selection then plated on LB agar containing 50 µg mL⁻¹ ampicillin. Positive clones were identified by PCR amplification using the plasmid-encoded M13F (5'-GTAAAAC-GACGGCCAG-3') and M13R (5'-CAGGAAACAGCTATGAC-3') primers, following the manufacturer's instructions and reducing the PCR reaction volume to 25 μ L. For each strain, at least two PCR products of the expected size were chosen for sequencing. Residual primers and dNTPs were removed by incubation for 15 min at 37 °C with 20 U of exonuclease I and 2 U of shrimp alkaline phosphatase (New England Biolabs, Ipswich, MA, USA) per 10 μL of PCR reaction (concentration >10 ng μL^{-1}), followed by 15 min at 80 °C to inactivate the enzymes. Sanger sequencing was performed at the Genomics Core Facility at Texas A&M University (Corpus Christi, TX, USA). Each product was sequenced in both the forward and reverse directions using the D1R and D2C primers, respectively. Sequences were processed using Geneious Prime 2022.2.2 (Dotmatics, Boston, MA) for visual inspection, quality trimming, assembly of consensus sequence, and identification by BLAST search. The sequences of all strains used in this study were deposited at the NCBI (Accession: OQ060507-OQ060514).

To further confirm the identification derived by BLAST search, sequences of strains analyzed in this study were compared to reference sequences of *Gambierdiscus* species via phylogenetic analysis. The analysis was conducted using Geneious 2022.2.2. Reference sequences for multiple *Gambierdiscus* species were aligned with the consensus sequences determined in this study using ClustalOmega 1.2.3. The resulting alignment was trimmed to remove regions that were not shared between all sequences. The trimmed alignment was then used to generate a Maximum Likelihood tree using RAXML 8.2.11, with parameters of GTR gamma I nucleotide model, the Rapid Bootstrapping and search for best-scoring ML tree algorithm, and 1000 bootstrap replicates (Stamatakis, 2014). The best-scoring maximum likelihood tree is shown in Supplemental Fig. 1.

2.3. Gambierdiscus cell pellet extraction

Quadruplicate 40 mL aliquots of the Gambierdiscus cultures were concentrated by centrifugation (3000×g, 10 min, 25 $^{\circ}$ C), the supernatant was discarded, and the resultant pellet stored at -20 °C until extraction. The replicate (n = 4) cell pellets of G. silvae 1602 SH-6, G. caribaeus BPAug08, and G. caribaeus USVI-08 were subjected to three rounds of freeze-thaw (-20 to 20 °C). Each pellet was then extracted with MeOH (5 mL) by sonication on ice five times for 1 min each, using a Cole-Parmer Ultrasonic Processor (20 kHz; Vernon Hills, IL, USA) with a pulsed setting (10 s on, 10 s off) and amplitude set at 30%. Following sonication, methanolic cell extracts were centrifuged at $3309 \times g$ for 10 min and 4 °C, and the supernatant retained. The residual pellets were re-extracted twice more in an identical manner, and the combined supernatants were evaporated under N $_2$ at 45 $^{\circ}$ C. The residues were diluted in MeOH (2 mL) for colorimetric mouse neuroblastoma assay utilizing MTT (N2a-MTT) and LC-HRMS analysis. The mean equivalent (eq.) number of cells per μ L of extract was 39 cells μ L⁻¹ for G. silvae 1602 SH-6, 20 cells μL^{-1} for G. caribaeus BPAug08, and 42 cells μL^{-1} for G. caribaeus USVI-08.

2.4. N2a-MTT assessment of Gambierdiscus strains

The *Gambierdiscus* spp. cellular extracts (n = 4 per strain) were evaluated for CTX-like Na_V activity by N2a–MTT. The assay employed ouabain to block the sodium/potassium ATPase pump in combination with veratrine to activate the Na_V channels. Veratrine is the alkaloid fraction of *Schoenocaulon officinale* and *Veratrum album*, which contains primarily the Na_V activating alkaloids veratridine and cevadine

(Honerjäger et al., 1982, 1992; Hare, 1996; Ulbricht, 1998) and veratrine has been show to be equivalent to veratridine for sodium channel activation in cell-based assays (David and Nicholson, 2004). The assay was used to select *Gambierdiscus* cultures with CTX-like Na_V-dependent activity for LC—HRMS screening for putative C-CTXs. The ability of this assay to detect CTX-like activity was verified using the commercially available CTX3C standard, where a dose–response reduction in cell viability was observed in the presence of ouabain and veratrine (+OV) and no effect on cell viability was observed in the absence of ouabain and veratrine (-OV) (Supplementary Fig. 2).

Each crude extract was evaporated under N_2 , diluted in 200 μ L of 5% FBS–RPMI growth medium, vortex-mixed for 3×30 s and 18-point 2-fold serial dilution series were prepared. Each dilution was assayed in triplicate wells within a plate and over at least two independent N2a cell lines (to avoid passage-specific effects), providing robust biological and technical replication. The Na_V-dependent (CTX-like) activity of the crude extracts of *G. silvae* 1602 SH-6, *G. caribaeus* BPAug08, and *G. caribaeus* USVI-08 were compared to two 9-point CTX3C standard curves. Maximal doses for each *Gambierdiscus* strain were 19 cells well⁻¹ (85 cells mL⁻¹) for *G. silvae* 1602 SH-6, 10 cells well⁻¹ (44 cells mL⁻¹) for *G. caribaeus* BPAug08, and 40 cells well⁻¹ for *G. caribaeus* USVI-08 (170 cells mL⁻¹).

On the day prior to performing the assay, N2a cells were harvested and cell abundance was determined by quantitative microscopy following staining with sterile filtered 0.4% trypan blue in PBS. A quality assurance criterion of <10% mortality was used to determine whether N2a cells could be used. At least two independent N2a cell strains (modified from ATCC stocks as described in the Supplementary Information) were used with the aim of reducing potential passagespecific effects. Following cell counts and viability assessment, N2a cells were diluted in 5% FBS-RPMI (150 000 cells mL⁻¹) and seeded into 96-well plates at 30 000 cells per well (200 μ L well⁻¹). After 18 h of growth, the plates were evaluated by microscopy to confirm 50-60% confluence across wells and between plates. Within each set of assay plates of a single cell line conducted on the same day, one full plate was dedicated as a dosing confluence control (DCC), one plate was dedicated as a final confluence control (FCC), and two plates were dedicated for CTX3C standards. DCC and FCC plates were used for quality assurance of N2a confluency confirmation by MTT assay prior to dosing (50-60% confluence) and final assay development (90-100% confluence), respectively (see supplementary information).

Aliquots (10 µL) of the serially-diluted extracts were dosed in triplicate to N2a cells in wells already containing 200 µL 5% FBS-RPMI and co-treated with either 20 μ L PBS (-OV) to evaluate the cellular response to extracts without OV (-OV), or with 20 µL OV (+OV; 0.22 mM ouabain and 0.02 mM veratrine). The final volume in assay wells was 230 μ L. A variety of quality controls were included in this process to ensure stable cellular response and assure data quality. Within each sample and standard plate these included: a no-cell control (230 µL PBS; n = 16), confluence controls (cells plus 230 μ L 5% FBS–RPMI, n = 14), -OV control (cells, 200 μL 5% FBS-RPMI, 30 μL PBS, n=3), +OVcontrols (cells, 200 μ L 5% FBS–RPMI, 10 μ L PBS, and 20 μ L OV, n = 3), and a CTX positive control (cells, 200 μL 5% FBS–RPMI, 20 μL OV, 10 μL 0.5 pg CTX3C, n=6). On each assay day, at least two CTX3C standard curves were also evaluated in parallel with a 20 pg starting dose. A 9point 2-fold dilution series (Wako-1; $0.2-87~\text{ng mL}^{-1}$) was prepared in 5% FBS-RPMI, and each dilution was analyzed in triplicate within a plate with and without OV (Bennett and Robertson, 2021).

Following dosing, the plates were incubated at 37 $^{\circ}$ C, 5% CO $_2$ for 18 h. Dosing suspensions were then removed from the plates, and 60 μL MTT (3.0 mM in 5% FBS–RPMI) added to each well. Plates were incubated at 37 $^{\circ}$ C, 5% CO $_2$ for 30 min, then the MTT was removed, and replaced with DMSO (100 μL). Plates were mixed on an orbital shaker for 5 min, and raw absorbance values were read on a BioTek Epoch plate reader (Agilent Technologies) at 570 nm. Data were only accepted if raw absorbance values were within 15% coefficient of variance (CV)

between replicates. All raw absorbance data from sample wells without OV (-OV) were normalized to the -OV control and all sample wells containing OV (+OV) were normalized to the +OV control to produce a percent control. Normalization to dosing controls is considered a best practice for MTT-based assays by producing more robust comparisons of dose–response data between assays, across labs, and across instrumentation (where OD $_{max}$ may differ depending on the optics), reagent differences and/or lots of standard (Carre \tilde{n} o et al., 2021). This approach provides a reliable characterization of cytotoxic effects while mitigating false negatives or false positives that can be masked when controls are not incorporated into the data analysis pipeline (Carre \tilde{n} o et al., 2021; Ghasemi et al., 2021).

Using the extract concentrations in cells μL^{-1} , and the aliquot volume, the log of the dose was plotted in cells mL^{-1} (in assay), and dose–response curves fitted to a variable slope model of the four-parameter logistic curve using GraphPad Prism (v9.3.1) to determine an IC₅₀ for each strain (equation provided in Supplementary Table 1). The IC₅₀ of the curves generated for extracts of *G. silvae* 1602 SH-6, *G. caribaeus* BPAug08, and *G. caribaeus* USVI-08 were then compared to the IC₅₀ from two nine-point standard curves of CTX3C assayed in triplicate wells each day, to estimate the CTX-like Na_V-dependent activity in CTX3C eq. cell⁻¹ or mL^{-1} of the three *Gambierdiscus* cultures.

2.5. Semi-preparative fractionation of C-CTX5

A sub-sample of methanolic extract (1.0 mL) of G. silvae (1602 SH-6) was evaporated under N₂ at 35 °C, water and diethyl ether (3 mL each) were added, the mixture was vortex-mixed, centrifuged at 260×g, and the diethyl ether layer was removed. The aqueous layer was re-extracted with 3 mL diethyl ether, centrifuged (260×g), and the combined ether fractions were evaporated to dryness at 35 $^{\circ}$ C. The residue was dissolved in H₂O-MeCN (1:1, 100 μL), and repeated injections (5 μL) were separated on a Kinetex F5 UHPLC column (100 \times 2.1 mm, 1.7 μ m; Phenomenex, Torrance, CA, USA) maintained at 50 °C. An Agilent semipreparative quaternary HPLC pump was used with gradient elution, and mobile phases were composed of H2O (A) and MeCN (B). The gradient (0.3 mL/min) was: 0-18 min, 30-60% B; 18-18.1 min, 60-99% B; 18.1–22 min, 99% B; followed by an 8 min re-equilibration at 30% B. Fractions were collected with an in-line Agilent fraction collector at 0.3 min intervals from 14 to 17 min and monitored for C-CTX5 by LC-HRMS. Fractions from 15.8 to 16.4 min contained predominantly C-CTX5 and were pooled, evaporated to dryness at 45 °C in a Savant SpeedVac (Thermo Fisher Scientific), and dissolved in H₂O-MeCN (1:1, 100 µL). This semi-purified C-CTX5 fraction contained no other detectable CTXs by LC-HRMS and was estimated to have a purity of >98% pure with respect to other putative C-CTX-like impurities (m/z)1000-1250), and was used for chemical reactions, microsome experiments, and N2a-MTT-based assessments. Two batches were prepared, with batch 1 used in the initial LC-HRMS characterization and N2a-MTT evaluation, and batch 2 used for all subsequent experiments (described below).

2.6. Chemical transformations of C-CTX5

2.6.1. Oxidation of C-CTX5 with periodic acid

An aliquot (5 $\mu L)$ of the semi-purified C-CTX5 was diluted with MeCN–H₂O (1:1; 45 $\mu L)$ and mixed with aqueous periodic acid (HIO₄) (2 μL , 50 mM). The sample was vortex-mixed (30 s) and, after 2 h at 25 °C, was analyzed by LC–HRMS.

2.6.2. Borohydride reductions of C-CTX5

An aliquot (5 μ L) of the semi-purified C-CTX5 was diluted with MeOH (45 μ L) and added to sodium borohydride (0.1 mg). The sample was allowed to react for 15 min and remaining borohydride was hydrolyzed by the addition of 2 μ L acetic acid, and analyzed by LC-HRMS. A second aliquot (5 μ L) of the semi-purified C-CTX5 was prepared in

MeCN (20 μ L), and sodium cyanoborohydride in water (1 mg mL⁻¹; 20 μ L) and 10% formic acid in H₂O (5 μ L) were added sequentially in the order listed, in an HPLC vial. The solution was vortex-mixed and held in the autosampler (10 °C) for 24 h until LC—HRMS analysis.

2.6.3. ¹⁸O-labeling of C-CTX5

An aliquot (5 μ L) of the semi-purified C-CTX5 was added to an HPLC vial and the solvent was evaporated under N₂. The residue was dissolved in MeCN- H_2^{18} O-formic acid (8:4:1 by volume; 50 μ L) and vortex-mixed for 1 min. The reaction mixture was allowed to sit at ambient temperature for 48 h. An aliquot (20 $\mu L)$ was removed and reacted with sodium borohydride (0.1 mg) for 15 min, and the solution was quenched with acetic acid (2 μ L). The 18 O-labeled C-CTX5 and the NaBH₄-reduced 18 Olabeled solutions were transferred to vial inserts for LC-HRMS analysis. Isotopic peak height profiles were collected from LC-HRMS full-scan mass spectra of the in-source adducts of the compounds of interest and used to calculate the incorporation of oxygen-18 into the compounds using the NRC Isotopic Enrichment Calculator (Version December 2021; currently available at https://metrology.shinyapps.io/i sotopic-enrichment-calculator with source code available from https:// github.com/meijaj/isotopic-enrichment-calculator) as described previously (Mudge et al., 2022a).

2.7. Fish liver microsome incubation of C-CTX5

An aliquot (50 µL) of the semi-purified C-CTX5 was evaporated to dryness (50 $^{\circ}$ C, N₂) and the residue dissolved in 20 μ L of 1:1H₂O–MeCN. Liver microsomes from emerald parrotfish (N. usta) and sheepshead (A. probatocephalus), prepared and characterized in previous work (Gwinn et al., 2021), were adjusted to 2 mg/mL microsomal protein in a volume of 250 µL of a reaction mixture containing an NADPH regenerating system (0.91 mM NADPH, 0.83 mM NADP+, 19.4 mM glucose 6-phosphate, and 9 mM MgCl₂·6H₂O in 0.05 M HEPES buffer, adjusted to pH 7.4) and 1 U mL $^{-1}$ glucose-6-phosphate dehydrogenase. Following preincubation (2 min), incubations were initiated by the addition of 5 µL of the semi-purified C-CTX5 solution to the microsomal suspension in a shaking water bath maintained at 25 °C. Samples were capped during incubation, and aliquots (75 μ L) were withdrawn after 0, 30, and 60 min and immediately added to equal volumes of ice-cold MeCN to terminate the enzymatic reactions. Samples were kept on ice until centrifugation at 20 000×g for 10 min at 4 °C to precipitate proteins, after which the supernatant was filtered at 20 000×g for 1 min at 4 °C (0.22 μm nylon Costar Spin-X filter; Corning Life Sciences, Corning, NY, U.S.A.), and the filtrate transferred to vial inserts for LC-HRMS analysis.

2.8. N2a-MTT assay of C-CTX5 and C-CTX1/2

Aliquots of semi-purified C-CTX1/2 from S. barracuda and S. cavalla (Mudge et al., 2022a) and semi-purified C-CTX5 from G. silvae 1602 SH-6 were analyzed by full-scan LC-HRMS and diluted in MeOH to give equivalent peak area responses for the two C-CTXs, where it was assumed that the LC-HRMS responses of the two compounds would be approximately equimolar because of the small difference in molecular structure. Aliquots (10 µL) of each semi-purified, peak-area-standardized fraction were evaporated under N2 and the residues dissolved in 5% FBS-RPMI (200 μL). Nine-point two-fold serial dilutions were prepared in 5% FBS-RPMI media from the C-CTX1 and C-CTX5 solutions and 10 µL aliquots of each were subsequently dosed in triplicate to N2a cells in wells containing 200 µL 5% FBS-RPMI and co-treated with either PBS (-OV), or OV (+OV). Four independent assays were conducted. Controls were as described in the N2a-MTT bioassay assessment of Gambierdiscus strains (Section 2.4). Two full CTX3C standard curves were prepared with a starting dose of 20 pg (Wako-2; concentration range 0.2–87 ng mL⁻¹), assayed and analyzed in triplicate wells within a plate on each day, as previously described in Section 2.4 (Bennett and Robertson, 2021). Raw absorbance data from sample wells without OV

(-OV) were normalized to the -OV control and all sample wells containing OV (+OV) were normalized to the +OV control to produce a percent control.

2.9. LC-HRMS analysis

Analyses were performed using an Agilent 1290 Inifinity II LC equipped with a binary pump, temperature controlled autosampler (10 °C) and temperature-controlled column compartment (40 °C) (Agilent Technologies, Missisauga, ON, Canada) coupled to a Q Exactive HF Orbitrap mass spectrometer (Thermo Fischer Scientific, Waltham, MA, USA) with a heated electrospray ionization probe (HESI-II). Chromatographic separation used a Kinetex F5 UHPLC column (100 \times 2.1 mm, 1.7 μ m) with gradient elution and mobile phases composed of 0.1% formic acid in H₂O (A) and 0.1% formic acid in MeCN (B). The gradient (0.3 mL min $^{-1}$) was: 0–18 min, 30–60% B; 18–18.1 min, 60–99% B; 18.1–22 min, 99% B; followed by an 8 min re-equilibration at 30% B.

Full-scan acquisition was performed with positive ionization with a mass range of m/z 1000–1250. The spray voltage of the source was +4.5 kV, with a capillary temperature of 340 °C. The sheath and auxiliary gas were set at 40 and 10 (arbitrary units). The probe heater temperature was set at 150 °C and the S-Lens RF level was set to 100. The mass resolution setting was 120 000 with an automatic gain control (AGC) target of 1×10^6 and a maximum injection time of 100 ms per scan.

Product-ion spectra were acquired using targeted parallel reaction monitoring (PRM) scan mode with an isolation window of 1 m/z. The resolution setting was 60 000 with an AGC target of 5 \times 10⁶ and a maximum injection time of 1000 ms with a normalized collision energy of 12 in positive mode. Extracted-ion chromatograms were obtained with a mass tolerance of ± 5 ppm.

All data presented on C-CTXs is, of necessity, qualitative due to the absence of reference standards. Known C-CTXs in the *Gambierdiscus* cultures and reaction solutions were confirmed by comparison of full scan-spectra, product ion spectra and retention times with naturally-incurred C-CTXs in extracts of tissues from confirmed ciguateric fish tissue, as well as published data. Data reported herein were above the detection limit, defined as an extracted ion (±5 ppm) peak with signal-to-noise greater than 3. Molecular formula assignments, ring double bond equivalents (RDBE) and mass error were evaluated within XCalibur V4.0 (Elemental Composition tab). Exact masses were extracted with a mass tolerance of ±5 ppm and a charge of +1. Isotope distribution calculations were performed with the NRC Molecular Formula Calculator (2022, https://metrology.shinyapps.io/molecular-formula-calculator/) as previously described (Mallia et al., 2019; Mudge et al., 2022b)

Gambierone and 44-methylgambeirone content was estimated using the LC–HRMS data using external calibration with commercially available reference materials. A 5-point calibration curve was generated with concentrations ranging from 0.02 to 1 μ g mL⁻¹. Peak areas were determined with extracted ion chromatograms of the [M + H]⁺ for gambierone and 44-methylgambierone at m/z 1025.4774 and m/z 1039.4931, respectively.

3. Results

3.1. Gambierdiscus spp. profiling, LC—HRMS screening and identification of C-CTX5

Three isolates of *Gambierdiscus* isolated from the U.S. Virgin Islands were isolated, cultured, and harvested in this study. One strain was identified as *G. silvae* and two strains were identified as *G. caribaeus* via DNA sequencing and phylogenetic analysis (Supplementary Fig. 1).

Given that C-CTX precursors that are transformed into C-CTX1/2 in fish have not previously been identified in *Gambierdiscus* and the possibility that the precursor analogue(s) could possess hydrophilic substituents such as glycosides or sulfates that could potentially be

metabolized by fish following consumption, liquid-liquid partitioning was not employed prior to assessing their CTX-like Na $_{\rm V}$ activity in the N2a-MTT bioassay. These cultures were selected due to their Na $_{\rm V}$ activity as well as the fact that they did not exhibit any non-specific activity when applied to -OV cells (i.e., they did not elicit cytotoxicity in the N2a cells without cotreatment with OV, something that could have confounded the screening) at the cellular concentrations applied during the assay (Fig. 2B, Supplementary Fig. 2). *G. silvae* 1602 SH-6, had the highest CTX-like activity per cell (1.4 \pm 0.2 pg CTX3C eq. cell $^{-1}$; Fig. 2B). *G. caribaeus* BPAug08 and *G. caribaeus* USVI-08 had approx. eight-fold (0.16 \pm 0.02 pg CTX3C eq. cell $^{-1}$) and 17-fold (0.08 \pm 0.01 pg CTX3C eq. cell $^{-1}$) lower CTX-like activity, respectively (Supplementary Fig. 2).

Methanolic extracts from these cultures were screened for known CTXs and related polyether compounds using LC-HRMS, C-CTX1/2 was detected in G. silvae 1602 SH-6 with a peak area approximately 10 times lower than was observed in the S. barracuda reference material. Gambierone was detected in all extracts (6.5 \pm 0.8 pg cell⁻¹ in *G. silvae* 1602 SH-6, 0.6 ± 0.2 pg cell⁻¹ in G. caribaeus BPAug08 and 9.8 ± 0.6 pg cell⁻¹ in G. caribaeus USVI-08). 44-Methylgambierone was detected in G. silvae 1602 SH-6 (0.15 \pm 0.03 pg cell $^{-1}$) and G. caribaeus BPAug08 at $(7.1 \pm 4.2 \text{ pg cell}^{-1})$. No other reported gambierone-related polyether compounds were detected in the extracts. The small peak area of C-CTX1/2 in the G. silvae 1602 SH-6 and the similarly low total gambierone content across the three Gambierdiscus isolates did not correlate with the observed high Nay-specific activity, suggesting the presence of additional CTX-like compounds. Because G. silvae 1602 SH-6 showed the highest CTX-like Na_V activity in vitro, this strain was initially examined by LC-HRMS and was the major focus of this study. A chromatographic peak eluting at 11.2 min (Fig. 2C), later identified as the novel C-CTX5, had an unusually broad peak shape, characteristic of C-CTX1/2 (Supplementary Fig. 3), whose peak shape has been attributed to rapid oncolumn epimerization of the ketal at C-56 in acidic mobile phase (Kryuchkov et al., 2020). The full-scan mass spectrum of the peak at 11.2 min had $[M + H]^+$ at m/z 1139.6170, consistent with a molecular formula of $C_{62}H_{91}O_{19}^+$ (Δ 1.8 ppm; Fig. 2E). The spectrum was dominated by an in-source water-loss ion at m/z 1121.6067 ($C_{62}H_{89}O_{18}^+$; Δ 1.1 ppm), and the assigned formulae were confirmed by isotope pattern analysis for the [M + H]+, in-source water-loss and adduct ions observed (Supplementary Fig. 4). The HRMS full-scan mass spectrum closely resembled that of C-CTX1/2 (Supplementary Fig. 4) and those of other reported full-scan spectra of C-CTX1/2 (Hamilton et al., 2002; Estevez et al., 2020, 2023; Kryuchkov et al., 2020), except that this compound had an accurate mass 2.0167 Da lower than the corresponding ions observed for C-CTX1/2. The elemental formula indicated the presence of two fewer hydrogen atoms and one additional RDBE in C-CTX5, relative to C-CTX1/2 (Supplementary Table 2). Based on peak area, C-CTX5 was approximately 15 times more abundant than C-CTX1/2 in the G. silvae 1602 SH-6 extract, assuming similar ionization efficiencies. C-CTX5 was also detected in G. caribaeus BPAug08 and USVI-08 at approximately 18and 130-fold lower abundance, respectively, than C-CTX5 in G. silvae 1602 SH-6 (Supplementary Fig. 3). Trace levels of C-CTX5 were detected in extracts of S. barracuda from the U.S. Virgin Islands at about 2-3% relative to the dominant C-CTX1/2 peak in the same extract (Supplementary Fig. 5; Supplementary Table 2).

Product-ion spectra were acquired for $[M+H-H_2O]^+$ (m/z 1121.6) of C-CTX5 (Fig. 2F), and compared to the MS/MS-spectra of C-CTX1/2 acquired under identical conditions (Supplementary Fig. 6). The fragmentation nomenclature developed for polyether ladder-framed molecules (Kryuchkov et al., 2020) was applied to the novel CTX and used to identify regions that were shared by, or different between, C-CTX1/2 and C-CTX5. There were many similarities in the spectra of C-CTX1/2 and C-CTX5. Product ions from m/z 100–400 were identical, suggesting that rings L–N of C-CTX1/2 were also present in C-CTX5. Prominent product ions observed from m/z 700–1100 for C-CTX5, including water losses, the s_{11} fragment at m/z 833.4469 ($C_{48}H_{65}O_{12}^+$, Δ –0.2 ppm), and

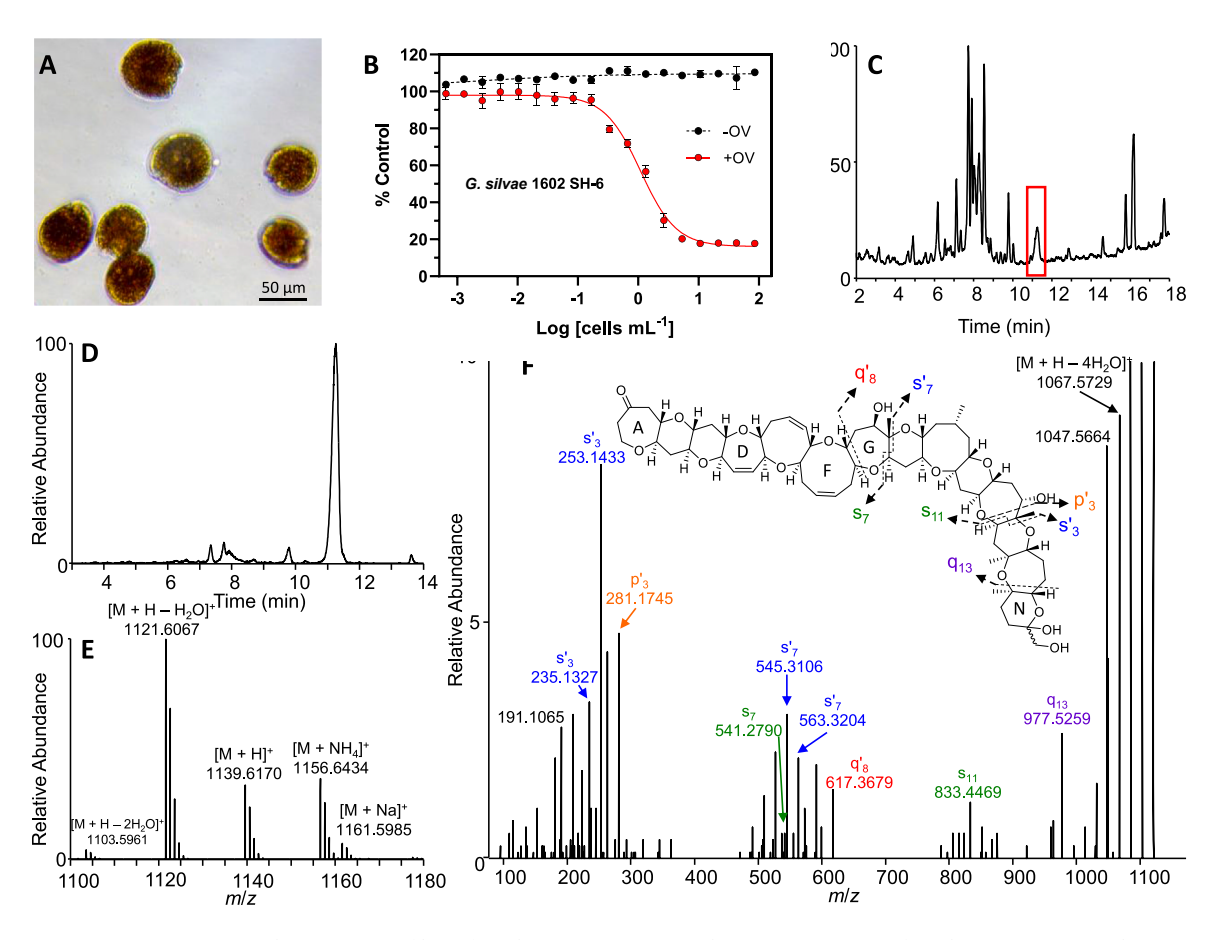


Fig. 2. Microscopy, N2a–MTT activity, and LC–HRMS profiling of G. silvae 1602 SH-6. (A) Light microscopy image of G. silvae 1602 SH-6 in culture. (B) Normalized N2a–MTT response (mean \pm SD) in cells sensitized with (+OV; red) and without (-OV; black) ouabain and veratrine, revealing the CTX-like response of the G. silvae 1602 SH-6 extracts dosed across a dilution series. (C) Total-ion chromatogram of G. silvae 1602 SH-6 extract (m/z 1000–1250), with the C-CTX5 peak marked in red. (D) Extracted-ion chromatogram of m/z 1121.6043 ([M + H-H₂O]⁺ for C-CTX5) in G. silvae 1602 SH-6. (E) Full-scan mass spectrum of C-CTX5 (m/z 1100–1180). (F) Product-ion spectrum of C-CTX5 [M + H - H₂O]⁺ (m/z 1121.6043), with identification of product-ions based on the proposed structure (3-oxoC-CTX1/2).

the q_{13} fragment at m/z 977.5259 ($C_{57}H_{77}O_{15}^+$, Δ 0.2 ppm), all had accurate masses consistent with two fewer hydrogen atoms and one extra RDBE relative to those of C-CTX1/2, further supporting the proposition that C-CTX5 is not modified in the L-N rings. The product ion spectra from m/z 400–700 showed several key distinguishing ions. The majority of these product ions were identical to those of C-CTX1/2, including all those attributable to the G-N rings. However, the fragment s_7 at m/z541.2790 ($C_{31}H_{41}O_8^+$, Δ 0.2 ppm) in C-CTX5 arising from fragmentation between rings G and H, is one of the few product ions originating from rings A-G. This fragment contained two fewer hydrogen atoms and one more RDBE than the corresponding ion from C-CTX1/2. Furthermore, the q'₈ fragment from C-CTX5 at m/z 617.3679 (C₃₅H₅₂O₉⁺, Δ -0.8 ppm) was identical to that from C-CTX1/2 at m/z 617.3682 ($C_{35}H_{52}O_9^+$, Δ -0.4 ppm). These results indicated that the difference between the two molecules was located in rings A-F. Based on the structure of C-CTX1/2, where rings D-F are already unsaturated, and the six-membered rings B and C are unlikely to contain a double bond (because this would result in unstable enol ethers), C-CTX1/2 and C-CTX5 most likely differed in their A-rings. Furthermore, the difference in retention times between C-CTX1/2 and C-CTX5 (8.7 vs 11.2 min) suggested the replacement of a polar functional group in C-CTX1/2 with a less polar group in C-CTX5.

The above considerations, and the fact that low levels of C-CTX1/2 were co-produced with C-CTX5 by G. silvae 1602 SH-6, led us to tentatively propose the structure for C-CTX5 shown in Fig. 1 (3-oxoC-CTX1/2). However, the possibility of an epoxide, or a 2,3- or 3,4-olefin in ring A together with a hydroxylation elsewhere in rings A–F, could not be

excluded based solely on the LC–HRMS/MS data. Therefore, a semi-purified fraction of the *G. silvae* 1602 SH-6 extract containing primarily C-CTX5, and no other identifiable CTX congeners, was used in a series of chemical reactions to verify the proposed C-CTX5 structure.

3.2. Structural confirmation of C-CTX5 with periodate, borohydride, and $H_2^{18}{\rm O}$ reactivity

The presence of a terminal diol at C-56/57 was confirmed by treating C-CTX5 with periodate, which rapidly cleaved the vicinal diol and resulted in the loss of CH₂O by forming a lactone with an observed m/z at 1107.5895 ($C_{61}H_{87}O_{18}^{+}$, Δ 0.7 ppm) in equilibrium with the corresponding hydroxy acid at m/z 1125.6001 ($C_{61}H_{89}O_{19}^{+}$, Δ 0.7 ppm) (Supplementary Fig. 7). This behaviour exactly paralleled the periodate cleavage of C-CTX1/2 (Kryuchkov et al., 2020), except that the two C-CTX5 reaction products each had two fewer hydrogen atoms and one more RDBE than the corresponding products from C-CTX1/2, consistent with the presence of the same N-ring in both C-CTX1/2 and C-CTX5.

Reduction with NaBH₄ has been reported to reduce the hemiketal at C-56 of C-CTX1/2 to produce semi-synthetic C-CTX3/4 (Kryuchkov et al., 2020). The reaction of C-CTX5 with NaBH₄ resulted in the formation of two sharp peaks with identical retention times and mass spectra to those of natural C-CTX3/4 in fish i.e., *S. barracuda* (Fig. 3A and B), with $[M + H]^+$ at m/z 1143.6473 ($C_{62}H_{95}O_{19}^+$, Δ 1.0 ppm) and m/z 1143.6476 ($C_{62}H_{95}O_{19}^+$, Δ 1.2 ppm), respectively. The addition of four hydrogen atoms to C-CTX5 indicated the presence of two reducible

sites in its structure, one of which was attributable to the C-56 hemiketal in the N-ring as described above. Furthermore, the conversion of C-CTX5 to C-CTX3/4, taken together with the LC-HRMS/MS data for C-CTX5, locates the second reducible site in ring A, consistent with a ketone, or possibly an epoxide, at C-3.

A less powerful reducing agent, NaBH3CN, was used to identify reaction intermediates between C-CTX5 and C-CTX3/4. After incubating semi-purified C-CTX5 for 24 h, four main products were observed (Fig. 3A), comprising: one broad peak of residual C-CTX5 $([M + H]^+)$ at m/z 1139.6163); two sharp peaks identical to those of C-CTX3/4 ([M + H]⁺ at m/z 1143.6466 and 1143.6473, respectively) and consistent with the products obtained following NaBH4 reduction; one broad peak identical to C-CTX1/2 ($[M + H]^+$ at m/z 1141.6320); and a fourth sharp, partially resolved peak at 8.9 min ([M + H] $^+$ at m/z 1141.6319; $C_{62}H_{93}O_{19}^{+}$, Δ 1.1 ppm), suggesting the absence of the epimerizable C-56 hemiketal. The accurate mass and derived molecular formula of this peak at 8.9 min were the same as for C-CTX1/2, but the adduct ion profile in the full-scan mass spectrum was similar to that of C-CTX3/4 (Supplementary Fig. 8A). The product ion spectrum of this compound indicated that reduction had occurred at the N-ring, with the C-3 ketone unreduced, suggesting that this peak originated from C-CTX5 that had been reduced at C-56 (i.e., 3-oxoC-CTX3/4) rather than at C-3 (Supplementary Figs. 8B-C).

Unlike hydroxy groups and epoxides, carbonyl groups (aldehydes, ketones, and carboxylic acids) and their equivalents (e.g., acetals, ketals, and enols) readily undergo acid-catalyzed exchange with labeled oxygen from water (Theodorou et al., 2014). Rapid acid-catalyzed ^{18}O -exchange was recently demonstrated at the C-56 ketal of C-CTX1/2 (Mudge et al., 2022a). When the same ^{18}O -exchange procedure was applied to the semi-purified C-CTX5, LC–HRMS analysis of the reaction mixture after 48 h indicated 64% and 80% ^{18}O -incorporation at two separate sites (C-3 and C-56), respectively, in C-CTX5, with [M + H] $^+$ at m/z 1143.6527 (C $_{62}H_{91}O_{17}^{18}O_{2}^{+}$, Δ 2.0 ppm) (Supplementary Fig. 9B). Subsequent reduction of this mixture with NaBH $_{4}$ afforded the two sharp peaks of $[^{18}O_{2}]\text{C-CTX3/4}$ with [M + H] $^+$ at m/z 1147.6565 and

1147.6564, respectively ($C_{62}H_{95}O_{17}^{18}O_{2}^{+}$, Δ 1.6 ppm and Δ 1.5 ppm) (Supplementary Fig. 9C), the isotope profiles of which indicated 96% ^{18}O -incorporation at both sites when analyzed with the NRC Isotope Enrichment Calculator. The reduction step permanently affixed the ^{18}O -labels to C-CTX3 and C-CTX4, so that on-column back-exchange could no longer occur, resulting in a higher percentage of labeling for the reduced product. This established the presence of two reducible carbonyl equivalents in C-CTX5, as compared to the single carbonyl equivalent present in C-CTX1/2. Furthermore, LC-HRMS/MS spectra of $[^{18}O_2]C$ -CTX3/4 were consistent with one of the labels being incorporated at rings A–F (Supplementary Fig. 10).

Thus, five lines of evidence establish C-CTX5 as 3-oxoC-CTX1/2: 1, the LC-HRMS/MS data indicated a gain of one RDBE and loss of 2H in rings A-F, compared to C-CTX1/2; 2, LC-HRMS data indicated that this change led to lower polarity; 3, periodate cleavage confirmed that the N-ring was consistent with that present in C-CTX1/2; 4, chemical reduction of C-CTX5 to C-CTX3/4 with borohydrides confirmed it as an analogue of C-CTX1-4 containing two reducible functional groups, and; 5, oxygen-18 labeling revealed the presence of two ketone equivalents in C-CTX5. These findings are also consistent with the observed co-production of C-CTX1 and C-CTX5 by *G. silvae*.

3.3. Biotransformation of C-CTX5 by fish liver microsomes

In vitro phase I metabolism of C-CTX5 was investigated using liver microsomes that were prepared and characterized during a previous study (Gwinn et al., 2021) from emerald parrotfish, N. usta, and sheepshead, A. probatocephalus, from the northern Gulf of Mexico. These species were chosen to represent lower and intermediate trophic levels i. e., herbivores and omnivores respectively, with parrotfish being a known CP vector (Gwinn et al., 2021). Semi-purified C-CTX5 was added to the liver microsomes in 60 min incubations under assay conditions previously optimized for phase I metabolism for both fish species (Gwinn et al., 2021). Incubation of C-CTX5 with N. usta microsomes did not result in a detectable reduction of the peak area of C-CTX5, but the

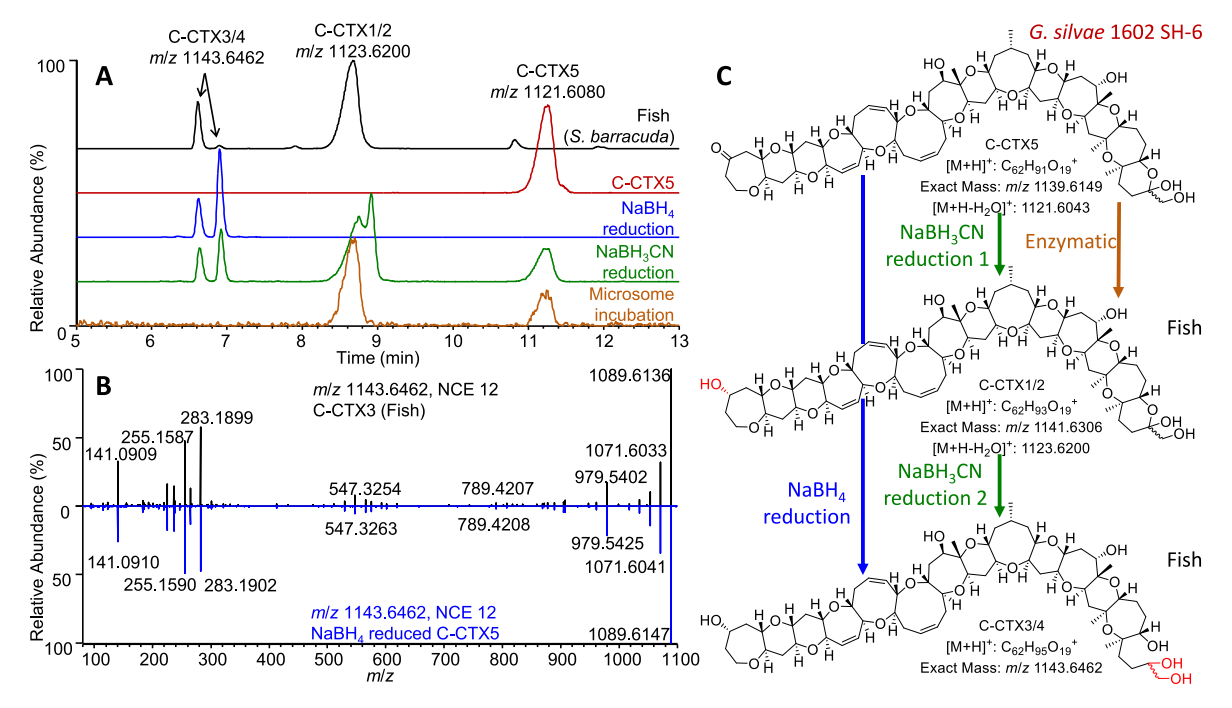


Fig. 3. Chemical and enzymatic conversions of C-CTX5 into known fish C-CTXs. (A) Overlaid extracted-ion chromatograms of C-CTX1/2 (m/z 1123.6200, [M + H-H₂O]⁺), C-CTX3/4 (m/z 1143.6462, [M + H]⁺) and C-CTX5 (m/z 1121.6043, [M + H-H₂O]⁺) in ciguatoxic fish (S. barracuda) from the Caribbean (black), semi-purified C-CTX5 isolated from G. silvae 1602 SH-6 (red), C-CTX5 chemically reduced with NaBH₄ (blue) and NaBH₃CN (green), and C-CTX5 metabolized with liver microsomes prepared from sheepshead (A. probatocephalus; amber). (B) Product-ion spectra of C-CTX3 from fish (black) and from NaBH₄ reduction of C-CTX5 (blue). (C) Scheme showing chemical and enzymatic reductions of C-CTX5 to known C-CTXs.

production of C-CTX1/2 at \sim 8% of the peak area of C-CTX5 after 60 min was observed (Supplementary Fig. 11B). This peak was at our established qualitative detection limit, at approximately 3 times the signal to noise. However, incubation with *A. probatocephalus* microsomes resulted in an 80% reduction of the C-CTX5 peak area over the course of the reaction and the concurrent appearance of C-CTX1/2. This peak was above the established detection limit with identical RT and mass spectra to C-CTX1/2 with a peak area response equivalent to \sim 60% of the initial C-CTX5 peak area (Fig. 3A, Supplementary Fig. 11). These incubations confirmed C-CTX5 as a precursor of C-CTX1/2 based on the enzymatic conversion in liver microsomes of fish from the Gulf of Mexico, and this biotransformation further verified the identity of C-CTX5 as 3-oxoC-CTX1/2.

3.4. Relative in vitro CTX-like Na_V bioactivity of C-CTX5 and C-CTX1/2

Due to the lack of available quantified C-CTX reference materials, solutions of semi-purified fractions of C-CTX1/2 isolated from fish and the semi-purified C-CTX5 from G. silvae 1602 SH-6 were prepared at equivalent peak-area-per-volume levels based on the response of the most dominant ion $([M + H - H₂O]^{+})$ in their respective LC-HRMS fullscan spectra. It was assumed that the LC-HRMS ionization efficiencies of the two compounds, and thus their analytical sensitivities, would be approximately equimolar because of the small difference in molecular structure. These semi-purified fractions were then used to evaluate their relative Na_V-dependent bioactivities using the N2a-MTT assay. C-CTX5 produced a CTX-like Na_V-specific response in cells sensitized with ouabain and veratrine (+OV), and had no effect on the viability of N2a cells in the absence of OV (-OV) (Fig. 4), as is expected for Na_V-activating toxins. Moreover, C-CTX5 and C-CTX1/2, dosed at equivalent peak-area-per-volume levels, produced dose-dependent reductions in the N2a response corresponding to IC50 values of 0.12 \pm 0.01 μL eq. for C-CTX1/2 and 0.28 \pm 0.03 μL eq. for C-CTX5 verifying that this novel CTX analogue has CTX-like Na_V activity using the N2a-MTT assay.

4. Discussion

The causative algae and the associated precursors of CTXs in Caribbean fish have not been identified. We hypothesized that Gambierdiscus spp. isolated from the Caribbean (St. Thomas, U.S. Virgin Islands) that exhibit CTX-like Na_V activity in vitro in the absence of non-specific activity could be profiled by LC-HRMS to identify potential precursor C-CTXs. The results showed that G. silvae and G. caribaeus isolates from the Caribbean produce C-CTX5 and that this compound is a precursor to C-CTX1/2 in fish, which is thought to be further metabolized to C-CTX3/4. Thus, C-CTX5 is a precursor to the CTX congeners dominant in toxic fish that cause CP in the Caribbean region. The novel Gambierdiscus toxin, C-CTX5, elicited a CTX-like response in a Na_V-specific in vitro assay using mouse neuroblastoma cells confirming a toxicological effect similar to that of C-CTX1/2, and was of the same order of magnitude. This is the first report of a confirmed algal C-CTX and significantly enhances the understanding of CP in the Caribbean and how it relates to the structurally similar Pacific CTXs.

While the biological role of C-CTX5 remains to be determined, the findings and methods presented here will allow targeted monitoring of C-CTXs in algae and fish. Importantly, while *G. silvae* has been identified as a toxigenic species (Robertson et al., 2018) and shown to exhibit CTX-like Nay-specific activity (Rossignoli et al., 2020), our confirmation of *G. caribaeus* as a producer of C-CTX5 also has significant implications for CP management. Until now, *G. caribaeus* has generally been regarded as having high proportional abundance (Lozano-Duque et al., 2018), but to be a minor toxin-contributing species within the epibenthic microalgal community assemblage throughout the Caribbean (Litaker et al., 2017; Pisapia et al., 2017a). While the two *G. caribaeus* strains evaluated here had lower CTX-like Nay activity than *G. silvae* 1602 SH-6, these are the most ciguatoxic strains based on CTX-like Nay activity of *G. caribaeus*

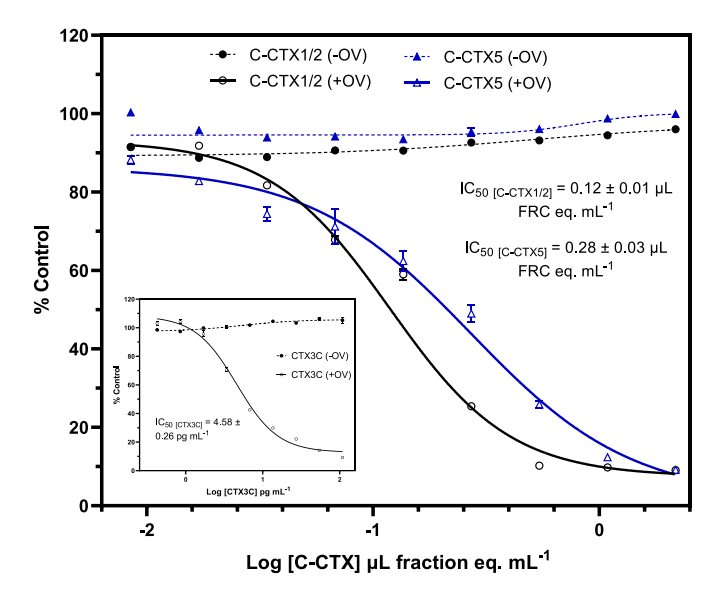


Fig. 4. CTX-like activity of semi-purified C-CTX1/2 (blue) and C-CTX5 (black) based on N2a–MTT activity with (+OV; solid lines), and without (-OV; dashed lines), ouabain and veratrine. Fractions (FRC) tested had approximately equivalent peak areas for each toxin based on LC–HRMS analysis. Data shown are the means of triplicate doses per treatment with standard error, across 9-point serial dilutions at approximate toxin equivalency across four independent assays.

that we have worked with to date. Caution should be taken in making comparisons to other studies due to differences in methodological approaches, geographical origin, and culture conditions, but G. caribaeus has been reported with toxin cell quotas ranging from 0.6 to 1.3 fg CTX3C eq. cell⁻¹ (approx. 130-fold lower than reported here) (Litaker et al., 2017) and 1-10 fg CTX3C eq. cell⁻¹ from 16 strains in our own G. caribaeus collections from the U.S. Virgin Islands (Robertson et al., 2018). The confirmation of G. caribaeus as a C-CTX5 producer and the high relative abundance of G. caribaeus in field samples from the U.S. Virgin Islands (M. Richlen, personal communication) suggests that this species could be a significant CTX source on the reef that would be available for subsequent trophic transfer. G. silvae 1602 SH-6 had a significantly higher Na_V bioactivity, as determined by N2a-MTT, and C-CTX5 content, as determined by LC-HRMS, than the two G. caribaeus strains, suggesting that G. silvae is also an important C-CTX producer in Caribbean reef ecosystems. With the identification of C-CTX5 and toxin-producing Gambierdiscus spp. from the Caribbean, it will be possible to compare Na_V bioactivities and C-CTX5 content across culture collections and in field samples to gain further insight into the distribution of C-CTXs. The measured in vitro Na_V bioactivities for G. excentricus VGO791 from the Canary Islands (1.43 pg CTX3C eq. cell⁻¹) (Pisapia et al., 2017a) suggests that this species may also be a significant toxin-contributor. Given that C-CTX1 has been reported in fish from the Canary Islands (Estevez et al., 2020), it is possible that C-CTX-5 or a related compound is also a contributing toxin in that species or other Gambierdiscus spp. in that region.

The major C-CTX congeners (C-CTX1/2) were first linked to reef fish and CP outbreaks in the Caribbean 25 years ago (Lewis et al., 1998), but C-CTXs have not been identified in algal sources until now. A putative I/C-CTX analogue was recently reported in a culture of *G. balechii* isolated from Indonesia with an accurate mass matching that of C-CTX1/2 (Tartaglione et al., 2023). However, the authors were unable to verify its identity with authentic standards and the full scan mass spectrum differed significantly from those for C-CTX1/2 presented here and in the literature (Vernoux and Lewis, 1997; Estevez et al., 2020, 2023; Kryuchkov et al., 2020). The identification of C-CTX5 herein provides unequivocal evidence of Caribbean *Gambierdiscus* spp. producing an

algal C-CTX precursor.

A significant body of work has been generated on Pacific CTXs due to the early identification of CTX4A/B and CTX3B/C produced by G. polynesiensis isolates (Satake et al., 1993, 1996) and of related CTX metabolites in fish (Murata et al., 1990; Yasumoto et al., 2000; Ikehara et al., 2017; FAO and WHO, 2020). Biotransformation studies of CTX4A/B and CTX3C in vitro and in vivo have shown that these toxins are metabolized into more oxidized forms (ie. CTX1B), resulting in more polar toxins with increased toxicity (Ikehara et al., 2017; FAO and WHO, 2020). While the transformation of C-CTX5 to C-CTX1/2 occurs via a reduction step rather than oxidation, an increase in polarity is observed. The detection of C-CTX1/2 at approximately 7% of the level of C-CTX5 in G. silvae suggests the presence of an oxido-reductase enzyme capable of reducing the C-3 ketone in the algae. C-CTX1/2 has consistently been reported as the dominant C-CTX in fish (Pottier et al., 2002a, 2002b; Abraham et al., 2012), therefore it is likely that fish take up C-CTX5 when consuming Gambierdiscus cells, that is then metabolized to C-CTX1/2, but a contribution from algal C-CTX1/2 can also be expected. Further research is necessary to identify the biochemical processes leading to the production, biotransformation and accumulation of these and other C-CTXs in marine ecosystems.

Additionally, several putative C-CTXs have been reported in fish harvested in the Caribbean that have been associated with suspected CP events (Pottier et al., 2002a, 2002b; Abraham et al., 2012). While in vitro toxicity was verified for many of the extracts, limited chemical formula and structural information was reported for these analogues (Pottier et al., 2002a, 2002b, 2003). Unfortunately, without additional MS/MS or structural data available it is impossible to deduce the possible structures of these compounds, or their possible relationship to confirmed C-CTXs such as C-CTX5. In previous reports of C-CTX profiles of naturally incurred fish tissues, C-CTX5 nor any analogues with an m/z1139.6 [M + H]⁺ ion have been reported. However, a putative Indian ciguatoxin (I-CTX5) was reported from a bull shark (Carcharhinus leucas) with an accurate mass consistent with the elemental composition of C-CTX5 (Diogène et al., 2017). The structural backbone of I-CTXs have not yet been elucidated, nor was any structural or MS/MS information presented on I-CTX5, so it is not possible to assess the properties of this putative I-CTX to those of C-CTX5. Similar techniques to those described herein for the identification of C-CTX5 using analytical scale materials could be useful in providing structural confirmation of putative CTXs in fish tissue and algal extracts.

The most toxic CTX by intraperitoneal injection in mice is the Pacific CTX1B, estimated to be approximately 10 times more potent than C-CTX1 and five times more potent than the algal CTX3C (FAO and WHO, 2020). While the *in vitro* N2a–MTT assay confirmed that C-CTX5 was ciguatoxic and that its IC $_{50}$ was about half that of C-CTX1/2, this was evaluated with the assumption of equimolar concentrations-based comparisons of peak-area-standardized semi-purified fractions. The Na_V potencies of both toxins will be evaluated quantitatively when appropriate purified reference materials become available.

C-CTX5 can be chemically and enzymatically converted into known fish metabolites associated with CP. The availability of an algal source of C-CTXs therefore has the potential to facilitate the production of analytical reference materials without the need to extract large quantities of naturally-incurred fish tissue. The majority of the data presented in this work are necessarily qualitative due to the absence of reference materials, however it is anticipated that the future production of quantitative materials will enable assay development and optimization, facilitate mechanistic and toxicokinetic studies of C-CTXs, and the development of diagnostic tests. Furthermore, the ability to introduce isotopic labels, like oxygen-18, as tracers into C-CTXs has the potential to significantly enhance future analytical and biochemical studies.

5. Conclusions

The identification of C-CTX5, and multiple lines of evidence

supporting it as a source of the CTXs associated with Caribbean CP, will transform management and monitoring approaches in endemic and emerging regions of concern. This will allow relevant spatiotemporal mapping of impacted coastal zones and development of data-informed predictive models to improve risk assessments. Ultimately, this will assist in preventing ciguatoxic fish from entering the market and reduce the incidence of CP in endemic regions.

Author contribution statement

Elizabeth M. Mudge: Conceptualization, Methodology, Investigation, Visualization, Writing – Original Draft, Writing – Review & editing, Christopher O. Miles: Conceptualization, Methodology, Supervision, Writing – Review & editing, Lada Ivanova: Investigation, Silvio Uhlig: Methodology, Investigation, Resources, Writing – Review & editing, Keiana S. James: Methodology, Investigation, Deana L. Erdner: Resources, Investigation, Funding acquisition, Christiane K. Fæste: Methodology, Writing – Review & editing, Pearse McCarron: Conceptualization, Resources, Supervision, Writing – Review & editing, Alison Robertson: Conceptualization, Methodology, Investigation, Resources, Visualization, Supervision, Writing – Original Draft, Writing – Review & editing, Project administration, Funding acquisition.

Funding

This work was supported through the National Science Foundation (NSF) Partnerships in International Research and Education Program (CiguaPIRE; 1743802) and contributes to the NSF and NIEHS Center for Oceans and Human Health: Greater Caribbean Center for Ciguatera Research (NSF: 1841811; and NIH: 1P01ES028949-01 to A.R., and D.L. E.). Additional support was through the National Oceanic and Atmospheric Administration National Centers for Coastal Ocean Science competitive research program under award NA11NOS4780028 (for A.R. and Florida Gulf Coast University) and is ECOHAB publication number ECO1027. NVI contributions were supported by a supplemental PIRE award through the Research Council of Norway (Grant No. 279247 to S·U.).

Declaration of competing interest

The authors declare that they have no known competing financial interests or personal relationships that could have appeared to influence the work reported in this paper.

Data availability

Data will be made available on request.

Acknowledgements

We thank Tyler B. Smith and Sarah Heidmann (University of the Virgin Islands) and their team for the collection and field processing of Dictyota from long-term monitoring sites in St. Thomas, U.S. Virgin Islands. We also thank Damon Freitag (University of Texas Marine Sciences Institute, Port Aransas, TX, USA) for performing cell counts associated with cultures harvested in this study, and Alex Elizabeth Murphy (University of South Alabama, Mobile, AL, USA) for maintenance and cryopreservation of N2a cultures. We are grateful to Jessica K. Gwinn (University of South Alabama, Mobile, AL, USA) for prior efforts including fish collection, liver microsome preparations used in this study, and microsome characterization that facilitated phase-I in vitro assessment of C-CTX5. We thank Fedor Kryuchkov (Norwegian Veterinary Institute, Ås, Norway) who performed C-CTX profiling in prior Bastille Day fish tissues by LC-HRMS. We appreciate the efforts of our collaborative partners including Michael L. Parsons, Rachael Schinbeckler, and Adam Catasus (Florida Gulf Coast University, Fort Myers,

FL, USA), and Mindy Richlen, Donald Anderson, and team (Woods Hole Oceanographic Institute, Woods Hole, MA, USA) for maintaining parallel *Gambierdiscus* culture collections, original isolation of *G. caribaeus* BPAug08, and contributing to both the original conception of this project and ongoing project development. We also thank D. Tim Harwood, Michael J. Boundy, and J. Sam Murray (Cawthron Institute, Nelson, New Zealand) for an in-house standard of 44-methylgambierone.

Appendix A. Supplementary data

Supplementary data to this article can be found online at https://doi.org/10.1016/j.chemosphere.2023.138659.

References

- Abraham, A., Jester, E.L.E., Granade, H.R., Plakas, S.M., Dickey, R.W., 2012. Caribbean ciguatoxin profile in raw and cooked fish implicated in ciguatera. Food Chem. 131, 192–198.
- Azziz-Baumgartner, E., Luber, G., Conklin, L., Tosteson, T.R., Granade, H.R., Dickey, R. W., Backer, L.C., 2012. Assessing the incidence of ciguatera fish poisoning with two surveys conducted in Culebra, Puerto Rico, during 2005 and 2006. Environ. Health Perspect. 120, 526–529.
- Bennett, C.T., Robertson, A., 2021. Depuration kinetics and growth dilution of Caribbean ciguatoxin in the omnivore *Lagodon rhomboides*: implications for trophic transfer and ciguatera risk. Toxins 13, 774.
- Boente-Juncal, A., Álvarez, M., Antelo, Á., Rodríguez, I., Calabro, K., Vale, C., Thomas, O. P., Botana, L.M., 2019. Structure elucidation and biological evaluation of maitotoxin-3, a homologue of gambierone, from *Gambierdiscus belizeanus*. Toxins 11, 79.
- Caillaud, A., De la Iglesia, P., Darius, H.T., Pauillac, S., Aligizaki, K., Fraga, S., Chinain, M., Diogène, J., 2010. Update on methodologies available for ciguatoxin determination: perspectives to confront the onset of ciguatera fish poisoning in Europe. Mar. Drugs 8, 1838–1907.
- Carreño, E.A., Alberto, A.V.P., de Souza, C.A.M., de Mello, H.L., Henriques-Pons, A., Anastacio Alves, L., 2021. Considerations and technical pitfalls in the employment of the MTT assay to evaluate photosensitizers for photodynamic therapy. Appl. Sci. 11, 2603.
- Chinain, M., Darius, H.T., Ung, A., Cruchet, P., Wang, Z., Ponton, D., Laurent, D., Pauillac, S., 2010. Growth and toxin production in the ciguatera-causing dinoflagellate Gambierdiscus polynesiensis (Dinophyceae) in culture. Toxicon 56, 739, 750
- Chinain, M., Gatti, C.M.i., Darius, H.T., Quod, J.P., Tester, P.A., 2021. Ciguatera poisonings: a global review of occurrences and trends. Harmful Algae 102, 101873.
- Darius, H.T., Revel, T., Viallon, J., Sibat, M., Cruchet, P., Longo, S., Hardison, D.R., Holland, W.C., Tester, P.A., Litaker, R.W., McCall, J.R., Hess, P., Chinain, M., 2022. Comparative study on the performance of three detection methods for the quantification of Pacific ciguatoxins in French Polynesian strains of *Gambierdiscus* polynesiensis. Mar. Drugs 20, 348.
- Darius, H.T., Roué, M., Sibat, M., Viallon, J., Gatti, C.M., Vandersea, M.W., Tester, P.A.,
 Litaker, R.W., Amzil, Z., Hess, P., Chinain, M., 2018. *Tectus niloticus* (Tegulidae,
 Gastropod) as a novel vector of ciguatera poisoning: detection of Pacific ciguatoxins
 in toxic samples from Nuku Hiva Island (French Polynesia). Toxins 10, 2.
- David, L.S., Nicholson, R.A., 2004. Quantitation of paralytic shellfish toxins using mouse brain synaptoneurosomes. Chemosphere 55, 1315–1321.
- Dechraoui, M.-Y., Naar, J., Pauillac, S., Legrand, A.-M., 1999. Ciguatoxins and brevetoxins, neurotoxic polyether compounds active on sodium channels. Toxicon 37, 125–143.
- Díaz-Asencio, L., Vandersea, M., Chomérat, N., Fraga, S., Clausing, R.J., Litaker, R.W., Chamero-Lago, D., Gómez-Batista, M., Moreira-González, A., Tester, P., Alonso-Hernández, C., Dechraoui Bottein, M.-Y., 2019. Morphology, toxicity and molecular characterization of *Gambierdiscus* spp. towards risk assessment of ciguatera in south central Cuba. Harmful Algae 86, 119–127.
- Diogène, J., Reverté, L., Rambla-Alegre, M., del Río, V., de la Iglesia, P., Campàs, M., Palacios, O., Flores, C., Caixach, J., Ralijaona, C., Razanajatovo, I., Pirog, A., Magalon, H., Arnich, N., Turquet, J., 2017. Identification of ciguatoxins in a shark involved in a fatal food poisoning in the Indian Ocean. Sci. Rep. 7, 8240, 8240.
- Doyle, J.J., Doyle, J.L., 1987. A rapid DNA isolation procedure for small quantities of fresh leaf tissue. Phytochem. Bull. 19, 11–15.
- Epelboin, L., Pérignon, A., Hossen, V., Vincent, R., Krys, S., Caumes, E., 2014. Two clusters of ciguatera fish poisoning in Paris, France, related to tropical fish imported from the French Caribbean by travelers. J. Trav. Med. 21, 397–402.
- Estevez, P., Oses Prieto, J., Burlingame, A., Gago Martinez, A., 2023. Characterization of the ciguatoxin profile in fish samples from the eastern Atlantic Ocean using capillary liquid chromatography-high resolution mass spectrometry. Food Chem. 418, 135960.
- Estevez, P., Sibat, M., Leão-Martins, J.M., Reis Costa, P., Gago-Martínez, A., Hess, P., 2020. Liquid chromatography coupled to high-resolution mass spectrometry for the confirmation of Caribbean ciguatoxin-1 as the main toxin responsible for ciguatera poisoning caused by fish from European Atlantic coasts. Toxins 12, 267.

FAO and WHO, 2020. Report of the Expert Meeting on Ciguatera Poisoning. Rome, 19–23 November 2018. Food Safety and Quality Series. World Health Organization, Rome. https://apps.who.int/iris/handle/10665/332640. (Accessed 24 March 2023).

- Friedemann, M., 2016. Erster ciguatera-ausbruch in deutschland 2012. Bundesgesundheitsblatt - Gesundheitsforsch. - Gesundheitsschutz 59, 1556–1565.
- Ghasemi, M., Turnbull, T., Sebastian, S., Kempson, I., 2021. The MTT assay: utility, limitations, pitfalls, and interpretation in bulk and single-cell analysis. Int. J. Mol. Sci. 22, 12827.
- Graber, N., Stavinksky, F., Hoffman, R., Button, J., Clark, N., Martin, S., Robertson, A., Hustedt, J., 2013. Ciguatera fish poisoning—New York city, 2010–2011. J. Am. Med. Assoc. 309, 1102–1104.
- Gwinn, J.K., Uhlig, S., Ivanova, L., Fæste, C.K., Kryuchkov, F., Robertson, A., 2021. In vitro glucuronidation of Caribbean ciguatoxins in fish: first report of conjugative ciguatoxin metabolites. Chem. Res. Toxicol. 34, 1910–1925.
- Hamilton, B., Hurbungs, M., Vernoux, J.-P., Jones, A., Lewis, R.J., 2002. Isolation and characterisation of Indian Ocean ciguatoxin. Toxicon 40, 685–693.
- Hare, J.D., 1996. Purification and quantitative analysis of veratridine and cevadine by HPLC. J. Agric. Food Chem. 44, 149–152.
- Holmes, M.J., Lewis, R.J., Poli, M.A., Gillespie, N.C., 1991. Strain dependent production of ciguatoxin precursors (gambiertoxins) by *Gambierdiscus toxicus* (Dinophyceae) in culture. Toxicon 29, 761–775.
- Holmes, M.J., Lewis, R.J., Sellin, M., Street, R., 1994. The origin of ciguatera in Platypus Bay, Australia. Memoir. Queensl. Mus. 34, 505–512.
- Honerjäger, P., Dugas, M., Zong, X.G., 1992. Mutually exclusive action of cationic veratridine and cevadine at an intracellular site of the cardiac sodium channel. J. Gen. Physiol. 99, 699–720.
- Honerjäger, P., Frelin, C., Lazdunski, M., 1982. Actions, interactions, and apparent affinities of various ceveratrum alkaloids at sodium channels of cultured neuroblastoma and cardiac cells. Naunyn-Schmiedeberg's Arch. Pharmacol. 321, 123–129.
- Ikehara, T., Kuniyoshi, K., Oshiro, N., Yasumoto, T., 2017. Biooxidation of ciguatoxins leads to species-specific toxin profiles. Toxins 9, 205.
- Keller, M.D., Selvin, R.C., Claus, W., Guillard, R.R.L., 1987. Media for the culture of oceanic ultraphytoplankton. J. Phycol. 23, 633–638.
- Kibler, S.R., Litaker, R.W., Holland, W.C., Vandersea, M.W., Tester, P.A., 2012. Growth of eight *Gambierdiscus* (Dinophyceae) species: effects of temperature, salinity and irradiance. Harmful Algae 19, 1–14.
- Kryuchkov, F., Robertson, A., Miles, C.O., Mudge, E.M., Uhlig, S., 2020. LC-HRMS and chemical derivatization strategies for the structure elucidation of Caribbean ciguatoxins: identification of C-CTX-3 and-4. Mar. Drugs 18, 182.
- Lewis, R.J., Inserra, M., Vetter, I., Holland, W.C., Hardison, D.R., Tester, P.A., Litaker, R. W., 2016. Rapid extraction and identification of maitotoxin and ciguatoxin-like toxins from Caribbean and Pacific *Gambierdiscus* using a new functional bioassay. PLoS One 11. e0160006.
- Lewis, R.J., Norton, R.S., Brereton, I.M., Eccles, C.D., 1993. Ciguatoxin-2 is a diastereomer of ciguatoxin-3. Toxicon 31, 637–643.
- Lewis, R.J., Vernoux, J.-P., Brereton, I.M., 1998. Structure of Caribbean ciguatoxin isolated from *Caranx latus*. J. Am. Chem. Soc. 120, 5914–5920.
- Liefer, J.D., Richlen, M.L., Smith, T.B., DeBose, J.L., Xu, Y., Anderson, D.M., Robertson, A., 2021. Asynchrony of *Gambierdiscus* spp. abundance and toxicity in the U.S. Virgin Islands: implications for monitoring and management of ciguatera. Toxins 13, 413.
- Litaker, R.W., Holland, W.C., Hardison, D.R., Pisapia, F., Hess, P., Kibler, S.R., Tester, P. A., 2017. Ciguatoxicity of *Gambierdiscus* and *fukuyoa* species from the caribbean and Gulf of Mexico. PLoS One 12, e0185776.
- Litaker, R.W., Vandersea, M.W., Faust, M.A., Kibler, S.R., Nau, A.W., Holland, W.C., Chinain, M., Holmes, M.J., Tester, P.A., 2010. Global distribution of ciguatera causing dinoflagellates in the genus *Gambierdiscus*. Toxicon 56, 711–730.
- Loeffler, C.R., Bodi, D., Tartaglione, L., Dell'Aversano, C., Preiss-Weigert, A., 2021. Improving in vitro ciguatoxin and brevetoxin detection: selecting neuroblastoma (Neuro-2a) cells with lower sensitivity to ouabain and veratridine (OV-LS). Harmful Algae 103. 101994.
- Loeffler, C.R., Spielmeyer, A., Friedemann, M., Kapp, K., Schwank, U., Kappenstein, O., Bodi, D., 2022. Food safety risk in Germany from mislabeled imported fish: ciguatera outbreak trace-back, toxin elucidation, and public health implications. Front. Mar. Sci. 9.
- Longo, S., Sibat, M., Viallon, J., Darius, H.T., Hess, P., Chinain, M., 2019. Intraspecific variability in the toxin production and toxin profiles of in vitro cultures of *Gambierdiscus polynesiensis* (Dinophyceae) from French Polynesia. Toxins 11, 735
- Lozano-Duque, Y., Richlen, M.L., Smith, T.B., Anderson, D.M., Erdner, D.L., 2018. Development and validation of PCR—RFLP assay for identification of *Gambierdiscus* species in the greater Caribbean region. J. Appl. Phycol. 30, 3529–3540.
- Mallia, V., Uhlig, S., Rafuse, C., Meija, J., Miles, C.O., 2019. Novel microcystins from Planktothrix prolifica NIVA-CYA 544 identified by LC-MS/MS, functional group derivatization and ¹⁵N-labeling. Mar. Drugs 17, 643.
- Mazzola, E.P., Deeds, J.R., Stutts, W.L., Ridge, C.D., Dickey, R.W., White, K.D., Williamson, R.T., Martin, G.E., 2019. Elucidation and partial NMR assignment of monosulfated maitotoxins from the Caribbean. Toxicon 164, 44–50.
- McMillan, J.P., Hoffman, P.A., Granade, H., 1986. *Gambierdiscus toxicus* from the Caribbean: a source of toxins involved in ciguatera. Mar. Fish. Rev. 48, 48–52.
- Morris, J.G., Lewin, P., Smith, C.W., Blake, P.A., Schneider, R., 1982. Ciguatera fish poisoning: epidemiology of the disease on St. Thomas, U.S. Virgin Islands. Am. J. Trop. Med. Hyg. 31, 574–578.
- Mudge, E.M., Meija, J., Uhlig, S., Robertson, A., McCarron, P., Miles, C.O., 2022a. Production and stability of oxygen-18 labeled Caribbean ciguatoxins and gambierones. Toxicon 211, 11–20.

- Mudge, E.M., Robertson, A., Leynse, A.K., McCarron, P., Miles, C.O., 2022b. Selective extraction of gambierone and related metabolites in *Gambierdiscus silvae* using maminophenylboronic acid-agarose gel and liquid chromatography-high-resolution mass spectrometric detection. J. Chromatogr., B: Anal. Technol. Biomed. Life Sci. 1188, 123014.
- Muecke, C., Hamper, L., Skinner, A.L., Osborne, C., 2015. Ciguatera fish poisoning in an international ship crew in Saint John Canada: 2015. Can. Comm. Dis. Rep. 41, 285–288.
- Murata, M., Legrand, A.M., Ishibashi, Y., Fukui, M., Yasumoto, T., 1990. Structures and configurations of ciguatoxin from the moray eel *Gymnothorax javanicus* and its likely precursor from the dinoflagellate *Gambierdiscus toxicus*. J. Am. Chem. Soc. 112, 4380–4386
- Pawlowiez, R., Darius, H.T., Cruchet, P., Rossi, F., Caillaud, A., Laurent, D., Chinain, M., 2013. Evaluation of seafood toxicity in the Australes archipelago (French Polynesia) using the neuroblastoma cell-based assay. Food Addit. Contam. 30, 567–586.
- Pisapia, F., Holland, W.C., Hardison, D.R., Litaker, R.W., Fraga, S., Nishimura, T., Adachi, M., Nguyen-Ngoc, L., Séchet, V., Amzil, Z., Herrenknecht, C., Hess, P., 2017a. Toxicity screening of 13 *Gambierdiscus* strains using neuro-2a and erythrocyte lysis bioassays. Harmful Algae 63, 173–183.
- Pisapia, F., Sibat, M., Herrenknecht, C., Lhaute, K., Gaiani, G., Ferron, P.-J., Fessard, V., Fraga, S., Nascimento, S.M., Litaker, R.W., Holland, W.C., Roullier, C., Hess, P., 2017b. Maitotoxin-4, a novel MTX analog produced by *Gambierdiscus excentricus*. Mar. Drugs 15, 220.
- Pottier, I., Hamilton, B., Jones, A., Lewis, R.J., Vernoux, J.P., 2003. Identification of slow and fast-acting toxins in a highly ciguatoxic barracuda (*Sphyraena barracuda*) by HPLC/MS and radiolabelled ligand binding. Toxicon 42, 663–672.
- Pottier, I., Vernoux, J.-P., Jones, A., Lewis, R.J., 2002a. Characterisation of multiple Caribbean ciguatoxins and congeners in individual specimens of horse-eye jack (*Caranx latus*) by high-performance liquid chromatography/mass spectrometry. Toxicon 40, 929–939.
- Pottier, I., Vernoux, J.-P., Lewis, R.J., 2001. Ciguatera fish poisoning in the caribbean islands and western Atlantic. Rev. Environ. Contam. Toxicol. 168, 99–141.
- Pottier, I., Vernoux, J.P., Jones, A., Lewis, R.J., 2002b. Analysis of toxin profiles in three different fish species causing ciguatera fish poisoning in Guadeloupe, French West Indies. Food Addit. Contam. 19, 1034–1042.
- Radke, E.G., Grattan, L.M., Cook, R.L., Smith, T.B., Anderson, D.M., Morris, J.G., 2013.
 Ciguatera incidence in the US Virgin Islands has not increased over a 30-year time period despite rising seawater temperatures. Am. J. Trop. Med. Hyg. 88, 908–913.
- Rhodes, L., Harwood, T., Smith, K., Argyle, P., Munday, R., 2014. Production of ciguatoxin and maitotoxin by strains of *Gambierdiscus australes, G. pacificus* and *G. polynesiensis* (Dinophyceae) isolated from Rarotonga, Cook Islands. Harmful Algae 39, 185–190.
- Robertson, A., Richlen, M.L., Erdner, D., Smith, T.B., Anderson, D.M., Liefer, J.D., Xu, Y., McCarron, P., Miles, C.O., Parsons, M.L., 2018. Toxicity, chemistry, and implications of *Gamberdiscus silvae*: a ciguatoxin superbug in the Greater Caribbean Region. In: Hess, P. (Ed.), 18th International Conference for Harmful Algae [Abstract Book]. International Society for the Study of Harmful Algae, Nantes, France, p. p115.

Rodríguez, I., Genta-Jouve, G., Alfonso, C., Calabro, K., Alonso, E., Sánchez, J.A., Alfonso, A., Thomas, O.P., Botana, L.M., 2015. Gambierone, a ladder-shaped polyether from the dinoflagellate *Gambierdiscus belizeanus*. Org. Lett. 17, 2392–2395. Rossignoli, E.A., Tudó, A., Bravo, I., Díaz, A.P., Diogène, J., Riobó, P., 2020. Toxicity

- characterisation of *Gambierdiscus* species from the canary islands. Toxins 12, 134. Satake, M., Fukui, M., Legrand, A.-M., Cruchet, P., Yasumoto, T., 1998. Isolation and
- Satake, M., Fukui, M., Legrand, A.-M., Cruchet, P., Yasumoto, T., 1998. Isolation and structures of new ciguatoxin analogs, 2,3-dihydroxyCTX3C and 51-hydroxyCTX3C, accumulated in tropical reef fish. Tetrahedron Lett. 39, 1197–1198.
- Satake, M., Ishibashi, Y., Legrand, A.-M., Yasumoto, T., 1996. Isolation and structure of ciguatoxin-4A, a new ciguatoxin precursor, from cultures of dinoflagellate Gambierdiscus toxicus and parrotfish Scarus gibbus. Biosci. Biotechnol. Biochem. 60, 2103–2105.
- Satake, M., Murata, M., Yasumoto, T., 1993. The structure of CTX3C, a ciguatoxin congener isolated from cultured *Gambierdiscus toxicus*. Tetrahedron Lett. 34, 1975–1978.
- Scholin, C.A., Herzog, M., Sogin, M., Anderson, D.M., 1994. Identification of group- and strain-specific genetic markers for globally distributed *Alexandrium* (Dinophyceae). II. Sequence analysis of a fragment of the LSU rRNA gene. J. Phycol. 30, 999–1011.
- Stamatakis, A., 2014. RAxML version 8: a tool for phylogenetic analysis and post-analysis of large phylogenies. Bioinformatics 30, 1312–1313.
- Tartaglione, L., Loeffler, C.R., Miele, V., Varriale, F., Varra, M., Monti, M., Varone, A., Bodi, D., Spielmeyer, A., Capellacci, S., Penna, A., Dell'Aversano, C., 2023.
 Dereplication of *Gambierdiscus balechii* extract by LC–HRMS and *in vitro* assay: first description of a putative ciguatoxin and confirmation of 44-methylgambierone. Chemosphere, 137940.
- Tester, P., Wickliffe, L., Jossart, J., Rhodes, L., Envoldsen, H., Adachi, M., Nishimura, T., Rodriguez, F., Chinain, M., Litaker, W., 2020. Global distribution of the genera *Gambierdiscus* and *fukuyoa*. In: Hess, P. (Ed.), Harmful Algae 2018—From Ecosystems to Socioecosystems. Proceedings of the 18th Intl. Conf. On Harmful Algae. International Society for the Study of Harmful Algae, Nantes France, pp. 21–26.
- Theodorou, V., Skobridis, K., Alivertis, D., Gerothanassis, I.P., 2014. Synthetic methodologies in organic chemistry involving incorporation of [¹⁷O] and [¹⁸O] isotopes. J. Labelled Compd. Radiopharm. 57, 481–508.
- Tosteson, T.R., 1995. The diversity and origins of toxins in ciguatera fish poisoning. Puert. Rico Health Sci. J. 14, 117–129.
- Ulbricht, W., 1998. Effects of veratridine on sodium currents and fluxes. Rev. Physiol. Biochem. Pharmacol. 133, 1–54.
- Vernoux, J.-P., Lewis, R.J., 1997. Isolation and characterisation of Caribbean ciguatoxins from the horse-eye jack (*Caranx latus*). Toxicon 35, 889–900.
- Villareal, T.A., Moore, C., Stribling, P., Van Dolah, F., Luber, G., 2006. Ciguatera fish poisoning — Texas, 1998, and South Carolina, 2004. Morb. Mortal. Wkly. Rep. 55, 935–937.
- Yasumoto, T., Igarashi, T., Legrand, A.-M., Cruchet, P., Chinain, M., Fujita, T., Naoki, H., 2000. Structural elucidation of ciguatoxin congeners by fast-atom bombardment tandem mass spectroscopy. J. Am. Chem. Soc. 122, 4988–4989.